ANALYSIS OF THE DUAL PHASE LAG BIO-HEAT TRANSFER EQUATION WITH CONSTANT AND TIME-DEPENDENT HEAT FLUX CONDITIONS ON SKIN SURFACE

by

Hamed ZIAEI POOR [a], Hassan MOOSAVI [a], and Amir MORADI [b*],

[a] Department of Mechanical Engineering, Isfahan University of Technology, Isfahan, Iran
[b] Department of Mechanical Engineering, Bu-Ali Sina University, Hamadan, Iran

Original scientific paper
DOI: 10.2298/TSCI140128057Z

This article focuses on temperature response of skin tissue due to time-dependent surface heat fluxes. Analytical solution is constructed for dual phase lag bio-heat transfer equation with constant, periodic, and pulse train heat flux conditions on skin surface. Separation of variables and Duhamel's theorem for a skin tissue as a finite domain are employed. The transient temperature responses for constant and time-dependent boundary conditions are obtained and discussed. The results show that there is major discrepancy between the predicted temperature of parabolic (Pennes bio-heat transfer), hyperbolic (thermal wave), and dual phase lag bio-heat transfer models when high heat flux accidents on the skin surface with a short duration or propagation speed of thermal wave is finite. The results illustrate that the dual phase lag model reduces to the hyperbolic model when τ_T approaches zero and the classic Fourier model when both thermal relaxations approach zero. However for $\tau_q = \tau_T$ the dual phase lag model anticipates different temperature distribution with that predicted by the Pennes model. Such discrepancy is due to the blood perfusion term in energy equation. It is in contrast to results from the literature for pure conduction material, where the dual phase lag model approaches the Fourier heat conduction model when $\tau_q = \tau_T$. The burn injury is also investigated.

Key words: *dual phase lag model, Laplace transform, skin tissue, thermal wave model, Fourier model*

Introduction

Analysis of heat transfer through biological materials like the skin tissue is very important not only for understanding of biological processes but also for many clinical applications such as cancer therapy, hyperthermia and cryopreservation [1, 2]. The skin is an extensive organ of living tissues which is made of three main compositions: epidermis, dermis, and subcutaneous tissue. The research of bioheat transfer was extended by advances in microwave, laser, and similar technologies. The accurate prediction of temperature response through biological tissues is very difficult due to the complex thermal interaction between vascular and extra-vascular systems. The accurate interpretation of bioheat transport through biological materials is very significant in many clinical procedures such as laser irradiation [3], hyperthermia [4],

* Corresponding author; e-mail: amir.moradi_hs@yahoo.com

and temperature-based diseases diagnostics [5]. During the past few decades, several researchers have presented analysis of bioheat transfer in the biological materials. Pennes [6] developed first bioheat transfer model of parabolic type in biological tissues. This model assumes that any thermal disturbance on a body is instantaneously felt throughout the body or the propagation speed of thermal waves is infinite. This model indicated some unrealistic results where the heat conduction behavior showed a non-Fourier or hyperbolic features like thermal wave phenomenon. After some experimental observations [7], interest on the non-Fourier or wave like feature of heat conduction was extremely increased. Cattaneo [8] and Vernott [9] presented a modification of Fourier's law as a linear extension of Fourier equation to describe the hyperbolic equation mathematically.

Liu *et al*. [10] firstly introduced a general model of the thermal wave model of bioheat transfer in living organs. The parabolic (Pennes bioheat transfer) model was used by various researchers to study bioheat transfer in biological soft tissues [11-13]. The thermal wave (hyperbolic) model of bioheat transfer in soft tissues was applied by some researchers to describe the thermal behavior of such organs. Different experiments on processed meat with different boundary conditions were carried out by Mitra *et al*. [14]. They observed wave-like features of heat conduction. Liu *et al*. [15] developed a newly thermal wave model to investigate the thermal damage of skin tissue. They analytically and numerically solved the parabolic and hyperbolic bioheat transfer equation for constant surface temperature and constant surface heat flux boundary conditions respectively. Xu *et al*. [16] first analytically solved the Pennes bioheat transfer equation (PBTE), thermal stress and thermal damage for a single-layer skin for different boundary conditions. They numerically solved the equations for a multi-layer skin. Liu *et al*. [17] extended a hybrid numerical scheme to solve the non-Fourier bioheat transfer equation for a multi-layer skin tissue. According to many experimental observations, thermal wave model produces more accurate anticipation than that of the Pennes bioheat transfer model. However some of its predictions do not agree with the experimental results [18, 19]. A study indicates that thermal wave model only considered the fast transient process of heat transfer but not the microstructural interactions. These two effects can be reasonably expressed by a dual phase lag (DPL) model and thus a phase lag for temperature gradient is introduced [20]. The DPL, hyperbolic and parabolic bioheat transfer models were used by Xu *et al*. [21] to model bioheat transfer across the tissue. They applied the finite difference scheme to solve the bioheat conduction equations numerically and finally found large discrepancies amongst anticipations of the Pennes, thermal wave and DPL models. Liu and Chen [22] employed the DPL model to interpret the non-Fourier thermal behavior of tissue during the hyperthermia treatment. Analysis of magnetic hyperthermia treatment using the DPL bioheat transfer model was carried out by Liu and Chen [23]. They eventually concluded that control of blood perfusion rate can help to have an ideal hyperthermia treatment. Zhang [24] performed an analysis of generalized DPL bioheat transfer equations based on non-equilibrium heat transfer in living biological tissues. He found that the lag times for living tissues are very close to each other. The DPL model was applied by Liu *et al*. [25] to analyze the bioheat transfer problem across skin tissue. They employed the DPL bioheat transfer model to study heat conduction across living tissues. As previously discussed, the temperature distribution and blood perfusion during surface heating have studied by many researchers. In the clinical applications, heat transfer often requires to simultaneously depend on transient and spatial heating both on the surface and inside biological bodies. Various researchers have carried out some efforts to analyze thermal behavior of living biological tissues for time-dependent surface heat flux conditions. Liu and Xu [26] represented a closed

analytical solution of Pennes bioheat transfer model for sinusoidal heat flux on the skin surface to estimate blood perfusion rate using phase shift between surface heat flux and surface temperature. Shih *et al.* [27] analytically solved the PBTE to analyze heat conduction across skin tissue with sinusoidal heat flux condition on skin surface. Ahmadikia *et al.* [28] developed an analytical solution via the Laplace transform method for the thermal wave model to investigate bioheat transfer problem across skin tissue during constant, pulse train and cosine heat flux conditions on skin surface. Horng *et al.* [29] investigated the effect of pulsatile of blood flow on thermal distribution during thermal therapy. They found that pulsatile velocity profile, with various combinations of pulsatile amplitude and frequency has little difference in effect on the thermal performance of tissue compared with uniform or parabolic velocity profile. Shih *et al.* [30] numerically studied the coupled effect of pulsatile blood flow and thermal relaxation time during thermal therapy. They found that the thermal behavior is quite insensitive to pulsation frequency in their study.

In this paper, we explore an analytical solution for the DPL bioheat transfer equation in skin tissue as a finite domain with the constant, cosine, and pulse train heat flux conditions on the skin surface. We constructed analytical solution by separation of variables method and Dumamel's theorem. The burn injury is also investigated here. This development in bioheat transfer problems of living biological tissues has not yet been pursued in the related literature. Most of reported analytical studies applied the Pennes bioheat transfer equation to study heat conduction problem across the skin with time-dependent heating conditions on skin surface.

Bioheat transfer models

The Pennes (Fourier) bioheat transfer model

The PBTE for biological tissues are well-known and is expressed [6]:

$$\rho_{\mathrm{t}} c_{\mathrm{t}} \frac{\partial T}{\partial t} = k \frac{\partial^2 T}{\partial x^2} + \rho_{\mathrm{b}} \varpi_{\mathrm{b}} c_{\mathrm{b}} (T_{\mathrm{a}} - T) + Q_{\mathrm{met}} + Q_{\mathrm{ext}} \tag{1}$$

Here ρ_{b} and c_{b} are the density and specific heat of the blood, respectively, ρ_{t}, c_{t}, and k are the density, specific heat, and thermal conductivity of skin tissue, respectively, ϖ_b – is the blood perfusion rate, T and T_{a} are skin tissue and blood temperatures, respectively, Q_{met} and Q_{ext} and the metabolic heat generation in skin tissue and the heat generated by external heating sources, respectively. In this study, Q_{ext} is zero.

Thermal wave model of bioheat transfer

The modification of classical Fourier's law by considering the concept of finite propagation speed of thermal waves was proposed by Vernott [8] and Cattaneo [9]:

$$q(x,t) + \tau_{\mathrm{q}} \frac{\partial q(x,t)}{\partial t} = -k \nabla T(x,t) \tag{2}$$

This constitutive relation is widely acceptable. Here $\tau_q > 0$ is a material property and is called the relaxation time. Considering eq. (2) for heat flux including relaxation time, τ_q, as well as the Pennes equation, a general form of thermal wave model of bioheat transfer in living biological tissues can be written [10]:

$$\tau_q \rho_{\mathrm{t}} c_{\mathrm{t}} \frac{\partial^2 T}{\partial t^2} + (\rho_{\mathrm{t}} c_{\mathrm{t}} + \tau_q \rho_{\mathrm{b}} \varpi_{\mathrm{b}} c_{\mathrm{b}}) \frac{\partial T}{\partial t} + \rho_{\mathrm{b}} \varpi_{\mathrm{b}} c_{\mathrm{b}} (T - T_{\mathrm{a}}) = k \frac{\partial^2 T}{\partial x^2} + \left(Q_{\mathrm{met}} + Q_{\mathrm{ext}} + \tau_q \frac{\partial Q_{\mathrm{met}}}{\partial t} + \tau_q \frac{\partial Q_{\mathrm{ext}}}{\partial t} \right) \tag{3}$$

where $\tau_q = \alpha/C^2$, α is the thermal diffusivity, and C – the thermal wave speed in the medium [14, 18].

Dual phase lag model of bioheat transfer

As discussed in introduction, the constitutive relation or thermal wave model has only considered fast transient process of heat transfer and has ignored the microstructural interactions. These two affects can be reasonably proposed by the DPL between q and ∇T, a further modification of the classical Fourier's model gives:

$$q(x,t) + \tau_q \frac{\partial q(x,t)}{\partial t} = -k\left[\nabla T(x,t) + \tau_T \frac{\partial \nabla T(x,t)}{\partial t}\right] \tag{4}$$

where τ_T is the relaxation time which is the phase-lag in establishing the temperature gradient across the medium during which conduction occurs through its small-scale structures. Based on eq. (4) for temperature gradient including the characteristic time, τ_T, as well as the thermal wave model of bioheat transfer equation, a general form of the DPL model of bioheat transfer in living tissues is expressed by [16]:

$$\begin{aligned} &\tau_q \rho_t c_t \frac{\partial^2 T}{\partial t^2} + (\rho_t c_t + \tau_q \rho_b \varpi_b c_b)\frac{\partial T}{\partial t} + \rho_b \varpi_b c_b (T - T_a) = \\ &= k\left(\frac{\partial^2 T}{\partial x^2} + \tau_T \frac{\partial^3 T}{\partial x^2 \partial t}\right) + \left(Q_{met} + Q_{ext} + \tau_q \frac{\partial Q_{met}}{\partial t} + \tau_q \frac{\partial Q_{ext}}{\partial t}\right) \end{aligned} \tag{5}$$

Analytical solution of DPL model of bioheat transfer equation

Here a closed form analytical solution of DPL bioheat transfer model is derived for the skin as a finite domain. Three types of boundary conditions are used on skin surface.

The solution of DPL model of bioheat transfer equation for constant surface heat flux condition on skin surface

The initial and boundary conditions for constant surface heating are expressed by:

$$T(x,0) = T_a, \qquad \left.\frac{\partial T}{\partial t}\right|_{t=0} = 0 \tag{6}$$

$$-k\left.\frac{\partial T}{\partial x}\right|_{x=0} = q_0, \qquad \left.\frac{\partial T}{\partial x}\right|_{x=l} = 0 \tag{7}$$

The dimensionless variables are defined:

$$\begin{aligned} &\xi = \sqrt{\frac{W_b c_b}{k}}\, x, \quad \theta = \frac{T - T_a}{q_0}\sqrt{k W_b c_b}, \quad \eta = \frac{W_b c_b}{\rho_t c_t} t, \quad \Lambda_q = \frac{W_b c_b}{\rho_t c_t}\tau_q, \\ &\Lambda_T = \frac{W_b c_b}{\rho_t c_t}\tau_T, \quad \psi = \frac{q_{met}}{q_0\sqrt{\frac{W_b c_b}{k}}}, \quad W_b = \rho_b \varpi_b, \quad L = \sqrt{\frac{W_b c_b}{k}}\, l \end{aligned} \tag{8}$$

Equation (5) (with respect to constant Q_{met} and $Q_{ext} = 0$) after arrangement can be re-written in terms of dimensionless variables:

$$\Lambda_q \frac{\partial^2 \theta}{\partial \eta^2} + (1 + \Lambda_q)\frac{\partial \theta}{\partial \eta} + \theta = \frac{\partial^2 \theta}{\partial \xi^2} + \Lambda_T \frac{\partial^3 \theta}{\partial \xi^2 \partial \eta} + \psi \tag{9}$$

The initial and boundary conditions in terms of dimensionless variables are:

$$\theta(\xi,0)=0, \qquad \left.\frac{\partial\theta}{\partial\eta}\right|_{\eta=0}=0 \tag{10}$$

$$\left.\frac{\partial\theta}{\partial\xi}\right|_{\xi=0}=-1, \qquad \left.\frac{\partial\theta}{\partial\xi}\right|_{\xi=L}=0 \tag{11}$$

This problem consists of non-homogeneous differential equation and non-homogeneous boundary condition on surface. Subsequently the problem is formulated in terms of a steady part and a transient part is:

$$\theta(\xi,\eta)=\theta_1(\xi,\eta)+\theta_2(\xi) \tag{12}$$

Substituting eq. (12) into eq. (9) yields:

$$\Lambda_q\frac{\partial^2\theta_1}{\partial\eta^2}+(1+\Lambda_q)\frac{\partial\theta_1}{\partial\eta}+\theta_1=\frac{\partial^2\theta_1}{\partial\xi^2}+\Lambda_T\frac{\partial^3\theta_1}{\partial\xi^2\partial\eta} \tag{13}$$

$$\frac{\partial^2\theta_2}{\partial\xi^2}-\theta_2=-\psi \tag{14}$$

The boundary conditions for steady-state part, eq. (14) are:

$$\left.\frac{\partial\theta_2}{\partial\xi}\right|_{\xi=0}=-1, \qquad \left.\frac{\partial\theta_2}{\partial\xi}\right|_{\xi=L}=0 \tag{15}$$

The solution for eq. (14) regarding the boundary conditions (15) is obtained by:

$$\theta_2(\xi)=\frac{\cosh(\xi-L)}{\sinh L}+\psi \tag{16}$$

Now the initial and boundary conditions for the transient part, eq. (13), are given by:

$$\theta_1(\xi,0)=-\theta_2(\xi), \qquad \left.\frac{\partial\theta_1}{\partial\eta}\right|_{\eta=0}=0 \tag{17}$$

$$\left.\frac{\partial\theta_1}{\partial\xi}\right|_{\xi=0}=0, \qquad \left.\frac{\partial\theta_1}{\partial\xi}\right|_{\xi=L}=0 \tag{18}$$

By considering boundary conditions (18), we expand the function $\theta_1(\xi,\eta)$ into the following Fourier series:

$$\theta_1(\xi,\eta)=\sum_{i=0}^{\infty}T_i(\eta)\cos\frac{i\pi}{L}\xi \tag{19}$$

Substitution of eq. (19) into eq. (13) gives:

$$\Lambda_q T_i''(\eta)+(1+\Lambda_q+\Lambda_T\lambda_i^2)T_i'(\eta)+(1+\lambda_i^2)T_i(\eta)=0, \qquad \lambda_i=\frac{i\pi}{L} \tag{20}$$

The general solution of differential eq. (20) is given by:

$$T_i(\eta)=a_i\ f_1(\eta,\lambda_i)+b_i\ f_2(\eta,\lambda_i) \tag{21}$$

By setting:

$$\Delta=(1+\Lambda_q+\Lambda_T\lambda_i^2)^2-4\Lambda_q(1+\lambda_i^2) \tag{22}$$

the functions f_1 and f_2 are expressed in the following fashion:

– if $\Delta > 0$

$$f_1(\eta,\lambda_i) = \mathrm{e}^{\frac{-(1+\Lambda_q+\Lambda_T\lambda_i^2)-\sqrt{\Delta}}{2\Lambda_q}\eta}, \quad f_2(\eta,\lambda_i) = \mathrm{e}^{\frac{-(1+\Lambda_q+\Lambda_T\lambda_i^2)+\sqrt{\Delta}}{2\Lambda_q}\eta} \tag{23}$$

– if $\Delta < 0$

$$f_1(\eta,\lambda_i) = \mathrm{e}^{\frac{-(1+\Lambda_q+\Lambda_T\lambda_i^2)}{2\Lambda_q}\eta}\cos\left(\frac{\sqrt{-\Delta}}{2\Lambda_q}\eta\right), \qquad f_2(\eta,\lambda_i) = \mathrm{e}^{\frac{-(1+\Lambda_q+\Lambda_T\lambda_i^2)}{2\Lambda_q}\eta}\sin\left(\frac{\sqrt{-\Delta}}{2\Lambda_q}\eta\right) \tag{24}$$

Employing the initial conditions (17) one has:

$$\sum_{i=1}^{\infty}\left[a_i\ f_1(0,\lambda_i) + b_i\ f_2(0,\lambda_i)\right]\cos(\lambda_i\,\xi) = -\theta_2(\xi) \tag{25}$$

$$\sum_{i=1}^{\infty}\left[a_i\frac{\partial f_1}{\partial\eta}(0,\lambda_i) + b_i\frac{\partial f_2}{\partial\eta}(0,\lambda_i)\right]\cos(\lambda_i\,\xi) = 0 \tag{26}$$

Solving the algebraic equation system (25) and (26) one arrives at:

$$\theta(\xi,\eta) = \frac{\cosh(\xi - L)}{\sinh L} + \psi + \left[a_0\ f_1(\eta,0) + b_0\ f_2(\eta,0)\right] + \\ + \sum_{i=1}^{\infty}\left[a_i\ f_1(\eta,\lambda_i) + b_i\ f_2(\eta,\lambda_i)\right]\cos(\lambda_i\,\xi) \tag{27}$$

The previous closed form analytical solution reduces to the thermal wave solution when $\Lambda_T = 0$.

The solution of DPL model of bioheat transfer for transient heat flux condition on skin surface

In the present study, the cosine heat flux is considered for transient heating condition on the skin surface. Here, the boundary condition on the skin surface should be only adapted according to cosine heat flux, thus it is expressed:

$$-k\left.\frac{\partial T}{\partial x}\right|_{x=0} = q_0\cos(\omega t) \tag{28}$$

where q_0 is the heat flux on the skin surface, and ω is the heating frequency. Other boundary condition and initial conditions are similar to that of the previous section In this type of heating, the dimensionless variables are defined:

$$\xi = \sqrt{\frac{\omega}{\alpha_1}}x, \quad \theta = \frac{k(T-T_\mathrm{a})}{q_0}\sqrt{\frac{\omega}{\alpha}}, \quad c_1 = \frac{W_\mathrm{b}c_\mathrm{b}}{\rho_\mathrm{t}c_\mathrm{t}\omega}, \\ \eta = \omega t, \quad \Lambda_q' = \omega\tau_q, \quad \Lambda_T' = \omega\tau_T, \\ \varphi = \frac{q_\mathrm{met}}{q_0\sqrt{\frac{\rho_\mathrm{t}c_\mathrm{t}\omega}{k}}}, \quad \alpha_1 = \frac{k}{\rho_\mathrm{t}c_\mathrm{t}}, \quad L = \sqrt{\frac{\omega}{\alpha_1}}l \tag{29}$$

Equation (5) with respect to the constant Q_met and $Q_\mathrm{ext} = 0$ and can be rewritten in terms of dimensionless variables:

$$\Lambda_q' \frac{\partial^2\theta}{\partial\eta^2} + (1 + c_1\Lambda_q')\frac{\partial\theta}{\partial\eta} + c_1\theta = \frac{\partial^2\theta}{\partial\xi^2} + \Lambda_T' \frac{\partial^3\theta}{\partial\xi^2\partial\eta} + \phi \tag{30}$$

The dimensionless form of surface boundary condition is:

$$\left.\frac{\partial\theta}{\partial\xi}\right|_{\xi=0} = -\cos(\eta) \tag{31}$$

Transient heat conduction problems with time-dependent boundary conditions or heat source cannot be solved by employing the separation of variables. Here the Durhamel's superposition integral with separation of variables is used. According to this method, continuous time-dependent disturbance is reduced to the sum of the time stepwise disturbances. So that, the general solution of $\theta(\xi,\eta)$ with reference to the time-dependent boundary condition $F(\eta) = \cos(\eta)$ is obtained with sum of stepwise solution of $\vartheta(\xi,\eta)$ in each step. With decreasing the time step $\mathrm{d}\tau$, the total effect at time η is achieved by integrating the effect of $F(\eta)$ in the time intervals of $\mathrm{d}\tau$ and summing it with the beginning effect of $F(0)$ [31]:

$$\theta(\xi,\eta) = F(0)\vartheta(\xi,\eta) + \int_0^\eta \vartheta(\xi,\eta-\tau)\frac{\mathrm{d}F(\tau)}{\mathrm{d}\tau}\mathrm{d}\tau \tag{32}$$

where $\vartheta(\xi,\eta)$ is the solution of eq. (30) with initial and boundary conditions (10) and (11). The function $\vartheta(\xi,\eta)$ is expressed by:

$$\vartheta(\xi,\eta) = \frac{\cosh\left[\sqrt{c_1}(\xi - L)\right]}{\sqrt{c_1}\sinh\left(\sqrt{c_1}L\right)} + \frac{\phi}{c_1} + \left[a_0\, f_1(\eta,0) + b_0\, f_2(\eta,0)\right] + \\ + \sum_{i=1}^{\infty}\left[a_i\, f_1(\eta,\lambda_i) + b_i\, f_2(\eta,\lambda_i)\right]\cos(\lambda_i\,\xi) \tag{33}$$

while the parameter Δ and functions f_1 and f_2 are defined by:

$$\Delta = (1 + c_1\Lambda_q + \Lambda_T\,\lambda_i^2)^2 - 4\,\Lambda_q\,(c_1 + \lambda_i^2), \qquad \lambda_i = \frac{i\,\pi}{L}$$

– if $\Delta > 0$

$$f_1(\eta,\lambda_i) = \mathrm{e}^{\frac{-(1+c_1\Lambda_q+\Lambda_T\,\lambda_i^2)-\sqrt{\Delta}}{2\Lambda_q}\eta}$$
$$f_2(\eta,\lambda_i) = \mathrm{e}^{\frac{-(1+c_1\Lambda_q+\Lambda_T\,\lambda_i^2)+\sqrt{\Delta}}{2\Lambda_q}\eta} \tag{34}$$

– if $\Delta < 0$

$$f_1(\eta,\lambda_i) = \mathrm{e}^{\frac{-(1+c_1\Lambda_q+\Lambda_T\,\lambda_i^2)}{2\Lambda_q}\eta}\cos\left(\frac{\sqrt{-\Delta}}{2\Lambda_q}\eta\right)$$
$$f_2(\eta,\lambda_i) = \mathrm{e}^{\frac{-(1+c_1\Lambda_q+\Lambda_T\,\lambda_i^2)}{2\Lambda_q}\eta}\sin\left(\frac{\sqrt{-\Delta}}{2\Lambda_q}\eta\right)$$

The coefficients a_i and b_i are calculated similar to that of the previous section. Now the solution of eq. (30) with time-dependent boundary condition (31) after utilizing eq. (32) is obtained by:

$$\theta(\xi,\eta)=\vartheta(\xi,\eta)-\int_0^{\eta}\vartheta(\xi,\eta-\tau)\sin(\tau)\,\mathrm{d}\tau \tag{35}$$

The solution of DPL model of bioheat transfer equation for the pulse train heat flux condition on skin surface

Common burns usually occur when skin is exposed to the high intensity heat flux in a short duration. Therefore to study the thermal behavior of skin, it is supposed the high intensity heat flux in a pulse time τ_i accidents to skin surface. The relevant boundary condition on skin surface is defined by:

$$-k\left.\frac{\partial T}{\partial x}\right|_{x=0}=q_0\left[U(t)-U(t-\tau_i)\right]h(t)=F(t) \tag{36}$$

where $U(t)$ is the unit step function and $h(t)$ is an arbitrary function which is set equal to one in this study. Here, again, we apply Duhamel's theorem to solve eq. (5) with time-dependent boundary condition (36) while the other boundary and initial conditions are similar to that of the previous section. For the piecewise continuous function $F(t)$, we have:

$$\begin{aligned}T(x,t)&=h(t)T(x,0)+\int_0^{t}\frac{\partial\bar{T}(x,t-\tau)}{\partial t}h(\tau)\mathrm{d}\tau,\quad t\le\tau_i,\\ T(x,t)&=h(t)T(x,0)+\int_0^{\tau_i}\frac{\partial\bar{T}(x,t-\tau)}{\partial t}h(\tau)\mathrm{d}\tau,\quad t>\tau_i\end{aligned} \tag{37}$$

In the previous equation the function $\bar{T}(x,t)$ is the solution of eq. (5) which has been expressed by eq. (27) if the dimensionless variables are replaced by the initial variables. The final solution of $T(x,t)$ with respect to the boundary condition, eq. (36), is:

$$\begin{aligned}T(x,t)&=T_{\mathrm{a}}+\int_0^{t}\frac{\partial\bar{T}(x,t-\tau)}{\partial t}\,\mathrm{d}\tau,\quad t\le\tau_i,\\ T(x,t)&=T_{\mathrm{a}}+\int_0^{\tau_i}\frac{\partial\bar{T}(x,t-\tau)}{\partial t}\,\mathrm{d}\tau,\quad t>\tau_i\end{aligned}$$

$$\begin{aligned}\bar{T}(x,t)=\frac{q_0}{\sqrt{kW_{\mathrm{b}}c_{\mathrm{b}}}}\Bigg\{&\frac{\cosh\left(\sqrt{\frac{W_{\mathrm{b}}c_{\mathrm{b}}}{k}}x-L\right)}{\sinh(L)}+\psi+\left[a_0\,f_1\left(\frac{W_{\mathrm{b}}c_{\mathrm{b}}}{\rho_{\mathrm{t}}c_{\mathrm{t}}}t,0\right)+b_0\,f_2\left(\frac{W_{\mathrm{b}}c_{\mathrm{b}}}{\rho_{\mathrm{t}}c_{\mathrm{t}}}t,0\right)\right]+\\ &+\sum_{i=1}^{\infty}\left[a_i\,f_1\left(\frac{W_{\mathrm{b}}c_{\mathrm{b}}}{\rho_{\mathrm{t}}c_{\mathrm{t}}}t,\lambda_i\right)+b_i\,f_2\left(\frac{W_{\mathrm{b}}c_{\mathrm{b}}}{\rho_{\mathrm{t}}c_{\mathrm{t}}}t,\lambda_i\right)\right]\cos\left(\lambda_i\sqrt{\frac{W_{\mathrm{b}}c_{\mathrm{b}}}{k}}x\right)\Bigg\}+T_a\end{aligned} \tag{38}$$

Analytical solution of the PBTE

The solution of PBTE for constant heating on skin surface

The solution of the Pennes bioheat transfer model in term of dimensionless variables (8) is obtained:

$$\theta(\xi,\eta)=\frac{\cosh(\xi-L)}{\sinh(L)}+\psi+\left[C_0\ f(\eta,0)\right]+\sum_{i=1}^{\infty}\left[C_i\ f(\eta,\lambda_i)\right]\cos(\lambda_i\xi),\quad \lambda_i=\frac{i\pi}{L}$$

$$C_i=\left(\frac{-2}{L}\right)\frac{\lambda_i+\left[\psi+\psi\,\lambda_i^2+\cosh(L)\lambda_i^2\right]\sin(\lambda_i L)}{\lambda_i+\lambda_i^3},\quad C_0=\frac{-1-L\psi}{\psi},\quad f(\eta,\lambda_i)=\mathrm{e}^{-\left(1+\lambda_i^2\right)\eta} \tag{39}$$

The solution of PBTE for transient heating on skin surface

The solution of the Pennes bioheat transfer model in term of dimensionless variables (29) is obtained:

$$\theta(\xi,\eta)=\vartheta(\xi,\eta)-\int_0^{\eta}\vartheta(\xi,\eta-\tau)\,\sin(\tau)\,\mathrm{d}\tau,$$

$$\vartheta(\xi,\eta)=\frac{\cosh\left[\sqrt{c_1}(\xi-L)\right]}{\sqrt{c_1}\sinh\left(\sqrt{c_1}\,L\right)}+\frac{\phi}{c_1}+D_0\ f(\eta,0)+\sum_{i=1}^{\infty}\left[D_i\ f(\eta,\lambda_i)\right]\cos(\lambda_i\xi), \tag{40}$$

$$f(\eta,\lambda_i)=\mathrm{e}^{-\left(1+\lambda_i^2\right)\eta},\qquad \lambda_i=\frac{i\pi}{L}$$

and the coefficients D_0 and D_i are calculated in the pattern of the previous section.

The solution of PBTE for pulse train heating on skin surface

The solution of the Pennes bioheat transfer model in term of dimensionless variables (8) is obtained:

$$T(x,t)=T_{\mathrm{a}}+\int_0^{t}\frac{\partial\overline{T}(x,t-\tau)}{\partial t}\,\mathrm{d}\tau,\quad t\le\tau_i,$$

$$T(x,t)=T_{\mathrm{a}}+\int_0^{\tau_i}\frac{\partial\overline{T}(x,t-\tau)}{\partial t}\,\mathrm{d}\tau,\quad t>\tau_i$$

$$\overline{T}(x,t)=\frac{q_0}{\sqrt{kW_{\mathrm{b}}c_{\mathrm{b}}}}\left(\begin{array}{l}\dfrac{\cosh\left(\sqrt{\dfrac{W_{\mathrm{b}}c_{\mathrm{b}}}{k}}x-L\right)}{\sinh L}+\psi+C_0\ \mathrm{e}^{-\frac{W_{\mathrm{b}}c_{\mathrm{b}}}{\rho_{\mathrm{t}}c_{\mathrm{t}}}t}+\\ +\displaystyle\sum_{i=1}^{\infty}C_i\ \mathrm{e}^{-\left(1+\lambda_i^2\right)\frac{W_{\mathrm{b}}c_{\mathrm{b}}}{\rho_{\mathrm{t}}c_{\mathrm{t}}}t}\cos\left(\lambda_i\sqrt{\frac{W_{\mathrm{b}}c_{\mathrm{b}}}{k}}x\right)\end{array}\right)+T_{\mathrm{a}} \tag{41}$$

where the coefficients C_0 and C_i are represented in eq. (39).

Thermal damage

In the burn evaluation, it is proven that thermal damage begins when the temperature at the basal layer, the interface between the epidermis and dermis increases above 44 ºC [32]. The evaluation of thermal damage is very important in bioengineering science of skin tissue

and clinical applications. The quantitative of thermal damage evaluation was initially suggested by Moritz and Henriques [33]. Such calculation was based on the fact that the tissue damage could be represented as an integral of a chemical process rate, *i. e.*:

$$\Omega = \int_0^t A\exp\left(-E_a/RT\right)\mathrm{d}t \tag{42}$$

where A is a material parameter equivalent to a frequency factor, E_a – the activation energy, and R = 8.313 J/mol. K – the universal gas constant. The constants A and E_a are experimentally obtained. For the first and second-degree of burns, T in eq. (42) is the basal layer temperature, while for the third-degree of burn, it is the temperature at the interface between dermis and subcutaneous layers (fat). The first and second-degree burns occur when both the conditions $T > 44$ °C and $\Omega > 0.53$ are satisfied in the basal layer. When $\Omega = 1$, the second-degree burn occurs [15].

Results and discussion

In this study, the temperature distribution through skin tissue is investigated for three models (Pennes, thermal wave and DPL) of bioheat transfer for three types of heat flux conditions on skin surface. The properties of skin tissue and blood are similar to that of reported by Xu *et al.* [21]. The relaxation time τ_q = 16 s [25] is considered for all analytical results here. The arterial temperature and blood perfusion rate are considered as T_a = 37 °C [21] and $W_b = \rho_b \varpi_b$ = 0.5 kg/m^3/s [26], respectively. A schematic domain of skin subjected to the boundary conditions is shown in fig. 1. Effect of the lag time, τ_T, on temperature profile when constant heat flux, q_0 = 5000 W/m^2 accidents to skin surface at the data frame DF interface is shown in fig. 2. It is noted that the discrepancy amongst bioheat transfer models increases, specially, at the initial times of heating when the heat flux intensity increases. As shown in fig. 2, for smaller relaxation times, τ_T, the DPL results approach the thermal wave outcomes. Further the Pennes bioheat transfer model gives higher prediction than that of thermal wave and DPL model due to infinite speed of heat propagation. Moreover, unlike the thermal wave model, no wave-like behavior is observed in the DPL model as expected, but a non-Fourier diffusion-like behavior is considered due to the second thermal relaxation, τ_T, whose influence weaken the thermal wave behavior. Further, unlike the pure conduction media, the DPL model predicts different temperature with that of Pennes model when $\tau_q = \tau_T$. This difference results from the blood perfusion rate in the energy equation of biological materials.

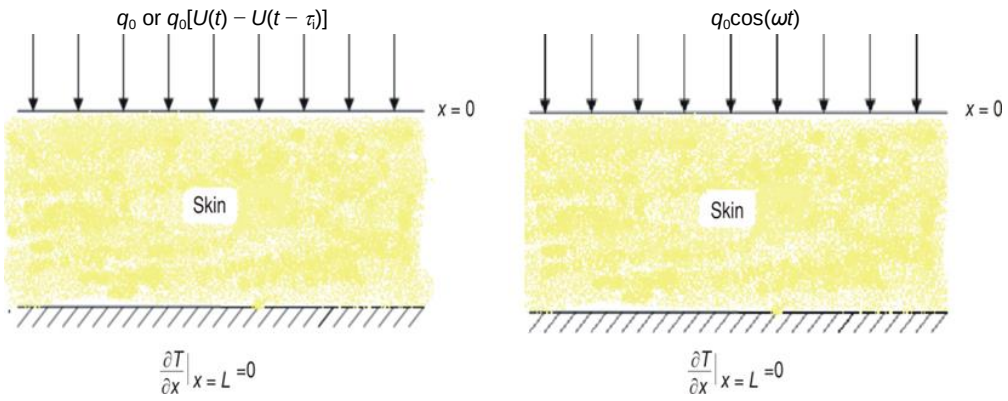

Figure 1. A schematic domain of skin tissue subjected to the boundary conditions

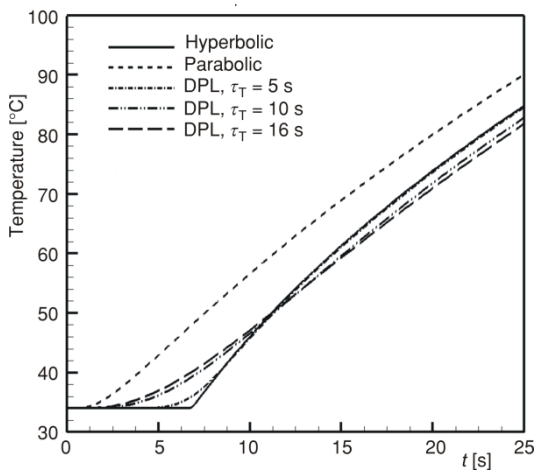

Figure 2. The temperature response for constant surface heating at DF interface when q_0 = 5000 W/m^2, τ_q = 16, τ_i = 1 s

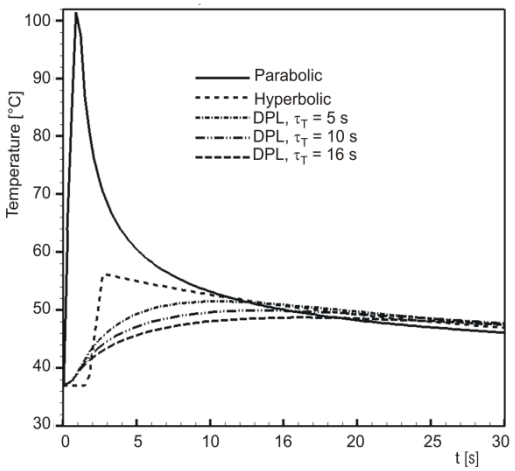

Figure 3. Temperature response for high power heat flux and short fire time duration at the basal layer when q_0 = 83200 W/m^2 τ_q = 16 s, τ_i = 1 s

There are many clinical applications where living biological tissues are exposed to the high intensity heat flux for the short duration of time. The temperature distribution for three bioheat transfer model when skin subjects to the heat flux q_0 = 83200 W/m^2 for time duration τ_i = 1s at the basal layer is shown in fig. 3. It is evident that there are major discrepancies among temperature predictions of three models in early times of heating when skin is exposed to the high intensity heat flux in short duration. It is also observed that when surface heat flux becomes zero after a short heating period, the elevated skin temperature from the Pennes model sharply decreases while times lag exist for the disappearance of heat flow from the thermal wave and DPL models. Further when $\tau_q = \tau_T$, the DPL results are substantially different from that of calculated by the Pennes model.

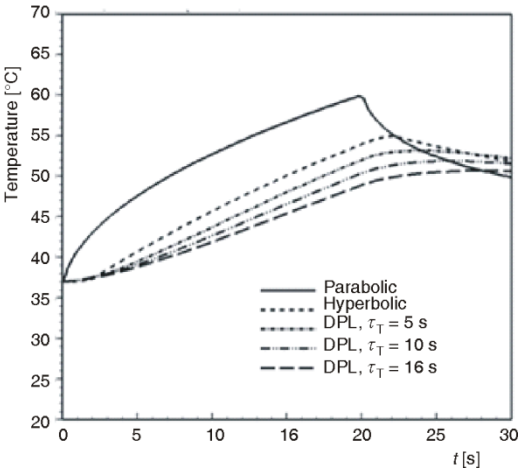

Figure 4. Temperature response for low power heat flux and longtime duration at the basal layer when q_0 = 5000 W/m^2, τ_q = 16 s, τ_i = 20 s

Figure 4 provides the temperature distribution for three bioheat transfer model when skin accidents to the surface heat flux q_0 = 5000 W/m^2 for time duration τ_i = 20 s at the basal layer. It is found that when heat flux is not intensive and duration of time increases, the lower discrepancies amongst the bioheat transfer models are observed. It should be noticed that the Pennes and thermal wave models of bioheat transfer anticipate the higher temperature than that of the DPL model during duration time. But after that the elevated skin temperature calculated by the Pennes model sharply decreases while the elevated skin temperatures calculated by the thermal wave and DPL models slowly decrease. Xu *et al.* [21] numerically solved the DPL bioheat transfer and found that similar results with those calculated in this study.

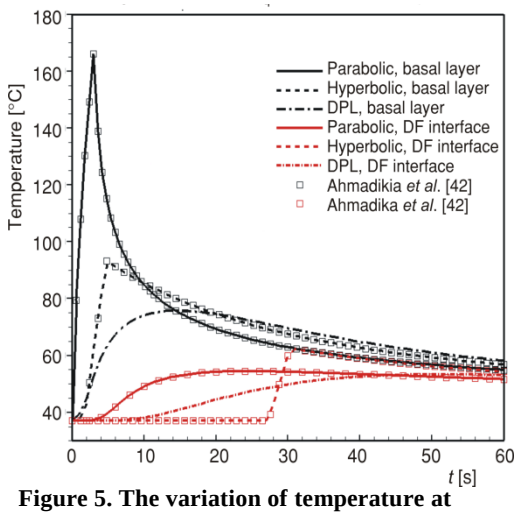

Figure 5. The variation of temperature at both ED and DF interfaces when the skin exposes to the propane gas flame for 3 s for q_0 = 83200 W/m^2 τ_q = 16 s, τ_T = 10 s

But they numerically solved the energy equation for a constant temperature at the skin surface. Qualitative comparison between the present DPL results (figs. 3 and 4) and those reported by Xu *et al*. [21] indicates that accuracy of the presented analytical solution in solution of DPL bioheat transfer equation. Comparison between bioheat transfer models when skin is exposed to the high intensity heat flux q_0 = 83200 W/m^2 for the time duration τ_i = 3 s at both basal layer and DF interface is depicted in fig. 5. This situation is similar to one where skin is exposed to the propane gas flame for 3 seconds [15]. Influence of thermal relaxation time, τ_q, is clearly observed because it takes 28 seconds for the thermal wave model to rise in order to be felt at the DF interface. While it only takes about 2 seconds and 8 seconds for the Pennes and DPL models, respectively. Here, the derived analytical results are also compared with those presented by Ahmadikia *et al*. [28] for both Pennes and thermal wave models and an excellent agreement is observed between the results (fig. 5). In this study, to investigate bioheat transfer with transient boundary condition on skin surface, the cosine heat flux with amplitude q_0 = 5000 W/m^2 is considered. Temperature response for three bioheat transfer models at the skin surface (x = 0) for ω = 0.1 is illustrated in fig. 6.

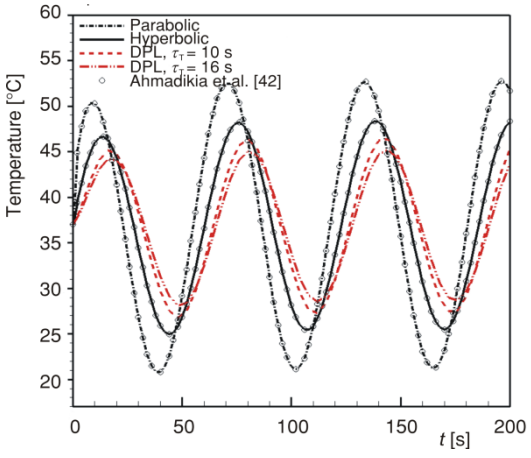

Figure 6. Temperature oscillation of three bioheat transfer model for both basal layer and DF interface when q_0 = 5000 W/m^2, ω = 0.1, τ_q = 16 s $q = q_0 \cos(\omega t)$

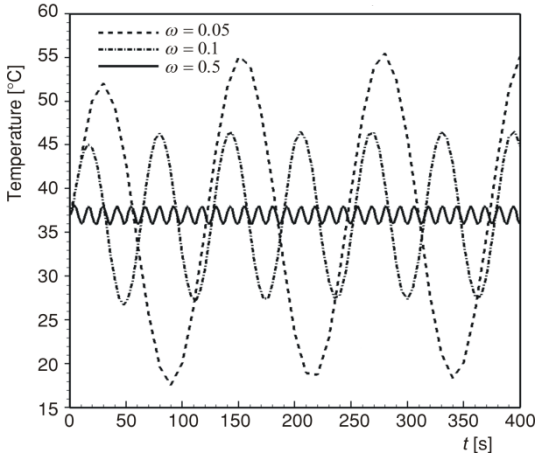

Figure 7. Temperature oscillation of the skin surface and different heat flux frequencies when q_0 = 5000 W/m^2, τ_q = 16 s, τ_T = 10 s, $q = q_0 \cos(\omega t)$

It is noted that the temperature amplitude for the thermal wave bioheat transfer model is larger and smaller than that of the DPL and Pennes models, respectively. It is also

seen that as the lag time, τ_T, increases the temperature amplitude becomes smaller. Even for the transient heat flux similar to the constant one the DPL model predicts completely different temperature with that of calculated by the Pennes equation when $\tau_q = \tau_T$. Moreover, the results of fig. 6 exhibit that there is a good agreement between the present results and those reported by Ahmadikia *et al*. [28] for the Pennes and thermal wave models. Generally, the thermal lag time, τ_T, gets smooth the temperature profile and decreases the effect of thermal wave (wave-like behavior) in temperature distribution. Fig. 7 shows the DPL temperature responses for different frequencies at the skin surface. It indicates that by increasing the frequency of transient heat flux, the temperature amplitude becomes smaller as well as the response cyclic time also becomes shorter.

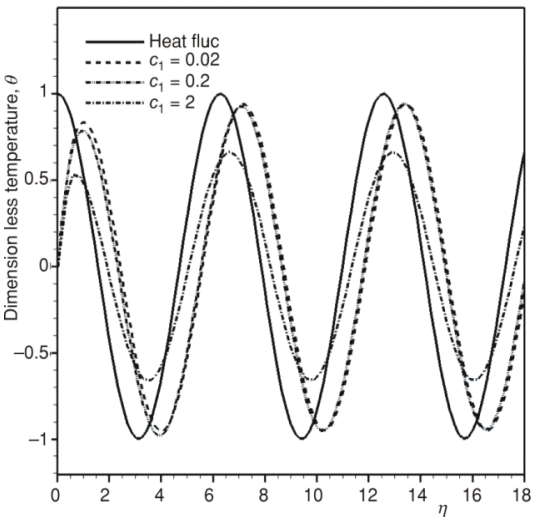

Figure 8. The variation of DPL dimensionless temperature for different values of dimensionless blood perfusion when q_0 = 5000 W/m^2, ω = 0.01, $q = q_0 \cos(\omega t)$ τ_q = 16 s, τ_T = 10 s

Figure 8 demonstrates the DPL dimensionless temperature oscillation at the skin surface for different values of the blood perfusion rate when $\omega = 0.01$ and $q_0 = 5000$ W/m^2 from $\eta = 0$ to $\eta = 18$. It is evident that for the lower blood perfusion rates ($c_1 = 0.02$ and $c_1 = 0.2$) there are not considerable changes between the temperature responses. Obviously, as the blood perfusion rate increases, the discrepancy between the temperature oscillations and heat flux gets more evident. It means that this method can be more suitable for perfusion measurement in highly perfused tissues. The higher frequency heat fluxes provides smaller temperature oscillations, thus the lower frequency heating would be more preferable due to its high sensitivity to blood perfusion rate. Effect of blood perfusion rate on the DPL temperature distribution of skin tissue at both ED (basal layer) and DF interfaces for constant surface heat flux $q_0 = 2000$ W/m^2 is illustrated in fig. 9. Clearly, the larger perfusion rates anticipate temperature response lower than that of the smaller one because further rate of blood perfusion can carry away the large amounts of heat. The history of temperature within skin depth when the skin is subjected to the propane gas flame is depicted in fig. 10. It is believed that the discrepancies amongst bioheat transfer models are more evident and large for the points closer to the skin surface, while these deviations decreases severely when heat propagates into the skin depth.

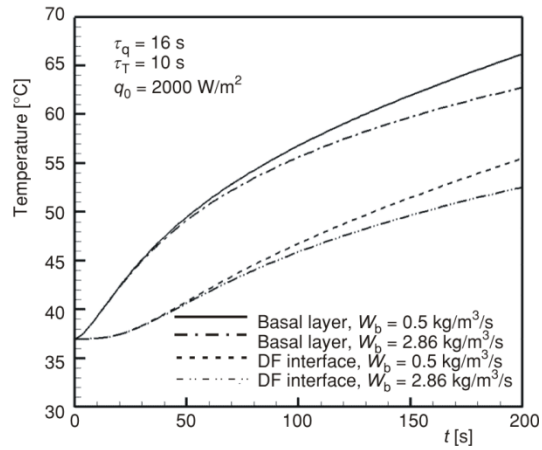

Figure 9. Temperature response of DPL model at for different values of blood perfusion rate when q_0 = 2000 W/m^2, τ_q = 16 s, τ_T = 10 s

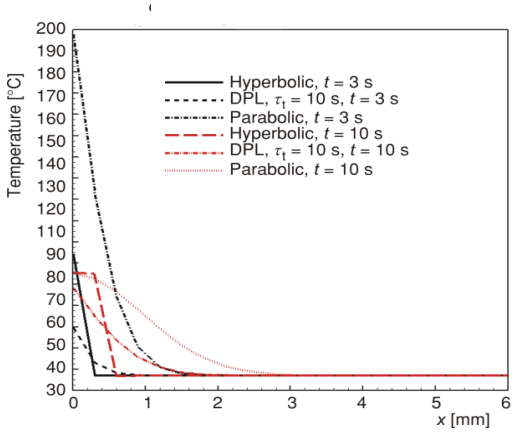

Figure 10. The variation of temperature along skin depth when the skin subjects to propane gas flame at different times when q_0 = 93200 W/m^2, τ_i = 3, τ_q = 16 s

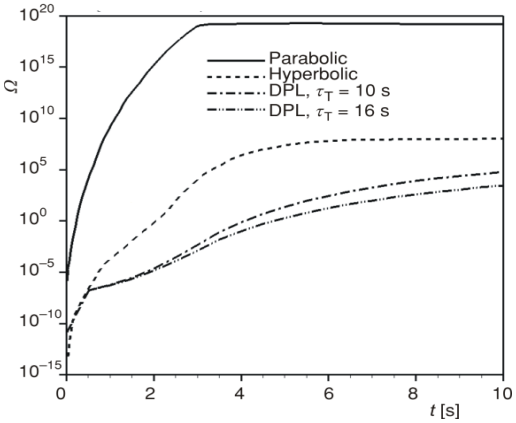

Figure 11. The variation of thermal damage at the basal layer when the skin subjects to propane gas flame (q_0 = 83200 W/m^2 τ_i = 3 s) for 3 seconds

Furthermore, for early times of heating, larger differences amongst heat transfer models are observed, while, as time goes on, these discrepancies drop considerably. The burn evaluation has always been and will continually be a significant problem in bioengineering science of skin tissue. The burn injury happens quickly and especially at the early stage of heating. Here, the thermal damage of skin tissue when skin is exposed to the propane gas flame q_0 = 83200 W/m^2 for 3 seconds for three bioheat transfer models is demonstrated in fig. 11. It is indicated that the burn time for DPL model is longer than that of other models. Further the burn time becomes longer as the value of thermal relaxation time, τ_T, gets larger. Figure 12 demonstrates the temperature response of tissue along the skin depth and time when skin is exposed to the propane gas for 3 seconds. As discussed in figs. 2-4 and 9, for the nearest points to the skin surface and early time of heating, discrepancies between the DPL and parabolic bioheat transfer models are great and these deviations decay as times goes on and heat propagates into the beneath layers of tissue. History of skin temperature along skin depth for three bioheat transfer models at different times when skin is subjected to constant heat flux q_0 = 5000 W/m^2 is illustrated in fig. 13. It can be clearly seen that the parabolic model predict higher temperature that that of DPL and thermal wave model for points closer to the surface. While heat propagates into skin depth, temperature obtained by the thermal wave model decreases abruptly to the core temperature, but temperature predicted by the DPL model decays slowly.

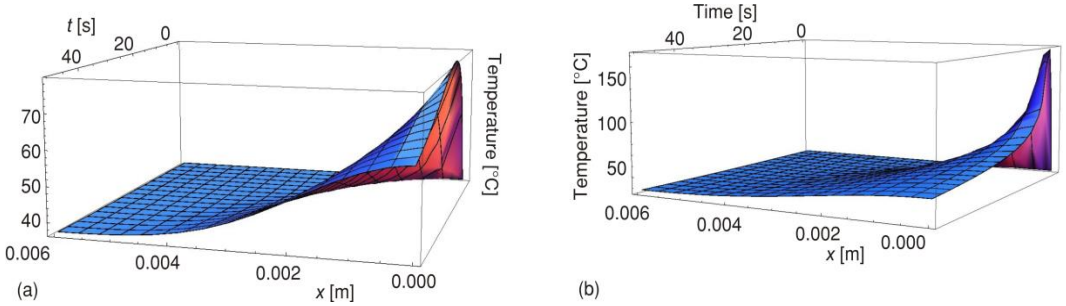

Figure 12. Temperature field *vs.* depth and time when q_0 = 83200 W/m^2, τ_i = 3, τ_q = 16 s, τ_T = 10 s

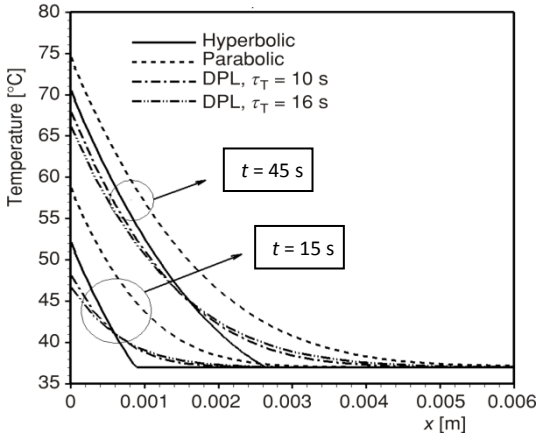

Figure 13. Temperature distribution along skin depth for constant heat flux q_0 = 5000 W/m^2 at different time when τ_q = 16 s

The qualitative comparison between fig. 13 with those calculated by Xu *et al*. [21] (fig. 6 in their paper) shows a good agreement and validates the present DPL results.

Conclusions

In this article, one dimensional DPL model of bioheat transfer equation for the single-layer skin tissue as a finite domain was analytically solved by employing the separation of variables and Duhamel's superposition integral. The analytical results for the continuous constant heat flux indicated that the larger deviation amongst predicted temperatures of the DPL, thermal wave and Pennes equations is found for intensive heat fluxes. The results demonstrated for fast heating with high intensity heat flux, large discrepancies are observed among the predicted temperatures by three models of bioheat transfer at early times of heating and points closer to the skin surface. Conversely for lower heat powers with long durations, predicted temperature by three bioheat transfer models are close to each other. The results exhibited both thermal relaxations τ_q and τ_T have significant effects on skin temperature. The thermal relaxation, τ_q, enforces the wave front phenomenon while it is smoothed by τ_T.

Unlike the pure conduction materials, the DPL bioheat transfer model calculates different temperature with that of the Pennes model when $\tau_q = \tau_T$. The derived analytical results for the transient heat flux condition showed that for the lower frequencies, the higher temperature amplitudes are noticed and such frequencies are more preferable because of its sensitivity to blood perfusion rate. It is found that the surface temperature of DPL model has larger phase shift with the surface heat flux and it increases as the value of τ_T becomes longer.

It is also found that three bioheat transfer models predict different burn time when the skin tissue is exposed to the propane gas flame for short duration.

References

[1] Cho, Y. I., *Bioengineering Heat Transfer*, *Advances in Heat Transfer*, Academic Press, London, Vol. 22, 1992
[2] Xu, F., *et al*., Mathematical Modeling of Skin Bioheat Transfer, *Appl. Mech. Rev*., *62* (2009), 5, pp. 050801-050836
[3] Jha, K. K., Narasimhan, A., Three-Dimensional Bio-Heat Transfer Simulation of Sequential and Simultaneous Retinal Laser Irradiation, *Int. J. Thermal Sciences*, *50* (2011), 7, pp. 1191-1198
[4] Zhu, L., *et al*., Quantification of the 3-D Electromagnetic Power Absorption Rate in Tissue during Transurethral Prostatic Microwave Thermotherapy Using Heat Transfer Model, *IEEE Tran. Biomed. Eng*., *45* (1998), 9, pp. 1163-1172
[5] Deng, Z. S., Liu, J., Mathematical Modeling of Temperature Mapping over Skin Surface and Its Implementation in Disease Diagnostic, *Computers in Biology and Medicine*, *34* (2004), 6, pp. 495-521
[6] Pennes, H. H., Analysis of Tissue and Arterial Blood Temperature in the Resting Forearm, *Journal of Applied Physiology*, *1* (1948), 2, pp. 93-122
[7] Peshkov, V., Second Sound in Helium II, *Journal of Physics*, *11* (1994), 3, pp. 580-584
[8] Cattaneo, C., A Form of Heat Conduction Equation which Eliminates the Paradox of Instantaneous Propagation, *Compte Rendus*, *247* (1958), pp. 431-433

[9] Vernotte, P., Paradoxes in Theory of Continuity for Heat Equation, *Compte Rendus*, *46* (1958), 22, pp. 3154-3155
[10] Liu, J., *et al*., Interpretation of Living Tissue's Temperature Oscillations by Thermal Wave Theory, *Chinese Science Bulletin*, *40* (1995), pp. 1493-1495
[11] Durkee Jr, J. W., *et al*., Exact Solutions to the Multiregion Time-Dependent Bioheat Equation. I: Solution Development, *Phys. Med. Biol*., *35* (1990), 7, pp. 847-867
[12] Foster, K. R., *et al*., Heating of Tissues by Microwaves: A Model Analysis, *Bioelectromagnetics*, *19* (1998), 7, pp. 420-428
[13] Shen, W., Zhang, J., Modeling and Numerical Simulation of Bioheat Transfer and Biomechanics in Soft Tissue, *Mathematical and Computer Modeling*, *41* (2005), 11-12, pp. 1251-1265
[14] Mitra, K., *et al*., Experimental Evidence of Hyperbolic Heat Conduction in Processed Meat, *Journal of Heat Transfer, Transactions of the ASME*, *117* (1995), 3, pp. 568-573
[15] Liu, J., *et al*., New Thermal Wave Aspects on Burn Evaluation of Skin Subjected to Instantaneous Heating, *IEEE Transaction on Biomedical Engineering*, *46* (1999), 4, pp. 4420-4428
[16] Xu, F., *et al*., Biothermomechanics of Skin Tissues, *Journal of the Mechanics and Physics of Solids*, *56* (2008), 5, pp. 1852-1884
[17] Liu, K. C., *et al*., Analysis of Non-Fourier Thermal Behavior for Multi-Layer Skin Model, *Thermal Science*, *15* (2011), 1, pp. 61-67
[18] Tzou, D. Y., *Macro-to Microscale Heat Transfer: The Lagging Behavior*, Taylor & Francis, Washington DC, USA, 1997
[19] Tzou, D. Y., A Unified Field Approach for Heat Conduction from Micro- to Macro-Scales, *J. Heat Transfer*, *117* (1995), 1, pp. 8-16
[20] Ozisik, M. N., Tzou, D. Y., On the Wave Theory in Heat Conduction, *J. Heat Transfer*, *116* (1994), 3, pp. 526-535
[21] Xu, F., *et al*., Non-Fourier Analysis of Skin Biothermomechanics, *Int. J. Heat and Mass Transfer*, *51* (2008), 9-10, pp. 2237-2259
[22] Liu, K. C., Chen, H. T., Investigation for the Dual Phase Lag Behavior of Bio-Heat Transfer, *Int. J. Thermal Sci*., *49* (2010), 7, pp. 1138-1146
[23] Liu, K. C., Chen, H. T., Analysis for the Dual-Phase-Lag Bio-Heat Transfer during Magnetic Hyperthermia Treatment, *Int. J. Heat and Mass Transfer*, *52* (2009), 5-6, pp. 1185-1192
[24] Zhang, Y., Generalized Dual-Phase Lag Bioheat Equations Based on Nonequilibrium Heat Transfer in Living Biological Tissues, *Int. J. Heat and Mass Transfer*, *52* (2009), 21-22, pp. 4829-4834
[25] Liu, K. C., *et al*., Investigation on the Bio-Heat Transfer with the Dual Phase-Lag Effect, *Int. J. Thermal Sci*., *58* (2012), Aug., pp. 29-35
[26] Liu, J., Xu, L. X., Estimation of Blood Perfusion Using Phase Shift in Temperature Response to Sinusoidal Heating at the Skin Surface, *IEEE Trans. Biomed. Eng*., *46* (1999), 9, pp. 1037-1043
[27] Shih, T. C., *et al*., Analytical Analysis of the Pennes Bioheat Transfer Equation with Sinusoidal Heat Flux Condition on Skin Surface, *Medical Engineering & Physics*, *29* (2007), 9, pp. 946-953
[28] Ahmadikia, H., *et al*., Analytical Solution of the Parabolic and Hyperbolic Heat Transfer Equations with Constant and Transient Heat Flux Conditions on Skin Tissue, *Int. Commun. Heat and Mass Transfer*, *39* (2012), 1, pp. 121-130
[29] Horng, T. L., *et al*., Effects of Pulsatile Blood Flow in Large Vessels on Thermal Dose Distribution During Thermal Therapy, *Med. Phys*., *34* (2007), 4, pp. 1312-1320
[30] Shih, T. C., *et al*., Numerical Analysis of Coupled Effects of Pulsatile Blood Flow and Thermal Relaxation Time During Thermal Therapy, *Int. J. Heat Mass Transfer*, *55* (2012), 13-14, pp. 3763-3773
[31] Arpaci, V. C., *Conduction Heat Transfer*, Addisson Wesley Publication, Boston, Mass., USA, 1966
[32] Torvi, D. A., Dale, J. D., A Finite Element Model of Skin Subjected to a Flash Fire, *J. Biomech. Eng*., *116* (1994), 3, pp. 250-255
[33] Moritz, A. R., Henriques, F. C., Study of Thermal Injuries II. The Relative Importance of Time and Source Temperature in the Causation of Cutaneous Burns, *American Journal of Pathology*, *23* (1947), 5, pp. 695-720

Paper submitted: January 28, 2014
Paper revised: April 8, 2014
Paper accepted: April 9, 2014